

Table of content

Table S1. Total (G+P) concentrations of PAHs [pg/m ³], %PM, and concentrations of OC and EC [μ g/m ³] measured in urban air of Longyearbyen in 2018.	2
Table S2. Total (G+P) concentrations of oxy-PAHs [pg/m ³] and %PM measured in urban air of Longyearbyen in 2018.	3
Table S3. Total (G+P) concentrations of nitro-PAHs [pg/m ³] and %PM measured in urban air of Longyearbyen in 2018.	4
Table S4. Sampling periods and air sample volumes.....	6
Table S5. 10-day backward trajectory probability analysis data.....	7
Table S6. Meteorological data for sampling days.....	8
Table S7. PAH concentrations (G+P; pg/m ³) in the air of Longyearbyen (UNIS) compared to the levels at the background Arctic stations in Svalbard and Finland measured during the same period in 2017/2018.....	9
Figure S1. Maps of the Arctic (a), Svalbard (b), vicinity of Longyearbyen (c), and marine traffic in Isfjorden (d) (North-West to the UNIS sampling station).	10
Figure S2. Sun diagram for Longyearbyen.....	11
Figure S3. Seasonal trends of weather parameters (a) and \sum_{20} PAH* total (G+P) concentrations measured in Svalbard air in 2018 at UNIS (Longyearbyen; urban) (b) and Zeppelin (Ny-Ålesund; background) (c) stations.	12
Figure S4. Synoptic map (a) and 10-day backward trajectories (b) illustrating frequent winter events of the Atlantic warm air masses transport to the Arctic.....	13
Figure S5. Wind rose diagrams typical for the P1-P3 cold (a) and P4 summer (b-c) periods.	14
Figure S6. Correlations of the OC/EC ratio and the sum gross tonnage of vessels.	15
Figure S7. Comparison of the P1-P3 cold period profiles of PAHs based on the snowmobile traffic intensity.	15
Figure S8. Comparison of the P4 summer profiles of PAHs based on wind direction (a) and the chemical profile proportion increase rates of PAHs (b) as result of ship traffic in the harbour of Longyearbyen.	16
Figure S9. Comparison of the P4 summer profiles of oxy-PAHs based on wind direction (a) and the chemical profile proportion increase rates of selected oxy-PAHs (with concentration > 10 pg/m ³) (b) as result of ship traffic (NW wind) in the harbour of Longyearbyen.	17
Figure S10. Comparison of the cold period P1-P3 profiles of oxy-PAHs based on snowmobile traffic intensity (a) and the chemical profile proportion increase rates of selected oxy-PAHs (with concentration > 10 pg/m ³) (b).	18
Figure S11. Comparison of the cold period P1-P3 profiles of nitro-PAHs based on the snowmobile traffic intensity (a) and the chemical profile proportion increase rates of selected nitro-PAHs (b).	19

Table S1. Total (G+P) concentrations of PAHs [pg/m³], %PM, and concentrations of OC and EC [μg/m³] measured in urban air of Longyearbyen in 2018.

Compound name	Abbreviated name	Cold period									Warm period				
		Dark winter P1 November-January n=8			Twilight winter P2 February n=4			Daylight spring P3 March-April n=7			%PM cold P1-P3 n=19	Polar day summer P4 May-June n=12			
		Mean	StDev	Median	Mean	StDev	Median	Mean	StDev	Median	Mean	Mean	StDev	Median	
Naphthalene	Nap	111.9	78.9	88.6	727.0	550.0	562.0	1533.0	760.0	1671.0	2.5	95.9	69.1	77.2	9.3
1-Methylnaphthalene	1-MeNap	58.1	27.6	56.0	336.5	159.6	276.3	890.0	389.0	744.0	7.8	105.6	65.7	80.8	38.2
2-Methylnaphthalene	2-MeNap	23.4	18.6	21.4	69.8	78.4	57.9	112.1	71.8	84.3	97.1	129.2	108.6	95.6	98.2
Acenaphthene	Ace	51.9	42.9	33.5	73.4	33.6	74.4	283.9	195.5	261.4	3.1	117.4	97.9	85.9	2.5
Fluorene	Flu	290.5	141.4	243.0	434.0	100.6	449.1	559.0	402.0	474.0	1.2	287.8	172.1	270.2	1.3
Phenanthrene	Phe	298.5	165.1	284.1	798.9	163.5	799.8	1129.0	594.0	1041.0	10.6	702.0	490.0	570.0	8.2
Anthracene	Ant	71.5	38.9	71.8	93.9	53.0	87.6	97.4	87.2	78.4	3.2	89.2	73.5	62.1	3.2
Fluoranthene	Flt	32.7	15.5	33.1	161.8	59.5	158.8	280.6	202.6	176.1	69.2	35.6	82.9	4.2	78.1
2-Methylfluoranthene	2-MeFlt	4.8	2.0	4.0	22.4	17.5	21.7	18.0	14.3	12.1	26.6	26.4	58.2	7.9	25.8
Pyrene	Pyr	34.7	21.0	32.8	95.5	63.3	116.1	154.8	76.9	155.2	48.9	84.6	78.0	69.1	15.4
Benzo[a]anthracene	BaAnt	3.9	0.3	4.0	1003.0	655.0	834.0	643.0	775.0	406.0	0.4	7.5	13.5	3.7	96.8
Chrysene	Chry	16.7	9.9	10.3	26.3	19.1	25.1	46.4	26.9	40.7	79.5	31.8	32.2	23.6	78.8
Retene	Ret	9.4	0.8	9.6	8.8	1.5	8.8	11.4	1.5	10.9	n.d.*	9.0	1.1	9.1	n.d.
Benzo[e]pyrene	BePyr	3.9	0.3	4.0	3.6	0.6	3.6	4.6	0.7	4.5	n.d.	5.2	3.7	3.8	n.d.
Benzo[j]fluoranthene	BjFlt	13.2	1.1	13.5	12.3	2.1	12.3	15.8	2.2	15.2	n.d.	12.6	1.5	12.7	n.d.
Benzo[b]fluoranthene	BbFlt	3.9	0.3	4.0	3.6	0.6	3.6	11.8	18.7	4.9	n.d.	3.7	0.5	3.7	n.d.
Benzo[k]fluoranthene	BkFlt	5.3	0.4	5.4	4.9	0.8	4.9	9.6	8.3	6.7	n.d.	6.4	5.0	5.1	85.6
Benzo[a]pyrene	BaPyp	5.5	4.2	4.0	12.2	9.5	11.8	11.1	10.8	5.4	93.8	8.5	9.3	3.9	93.5
Dibeno[a,h]anthracene	DBahAnt	11.4	21.3	4.0	3.6	0.6	3.6	4.6	0.7	4.5	97.7	3.7	0.5	3.7	n.d.
Benzo[g,h,i]perylene	BghiP	3.9	0.3	4.0	13.3	10.9	12.2	40.0	30.3	34.6	94.7	4.8	3.6	3.8	93.5
Indeno[1,2,3-cd]pyrene	IPyr	9.0	0.7	9.2	8.4	1.4	8.4	19.6	22.8	11.5	n.d.	8.6	1.1	8.7	n.d.
Coronene	Cor	3.9	0.3	4.0	9.8	6.9	8.7	27.3	32.2	5.5	94.0	3.7	0.5	3.7	n.d.
Σ22 PAHs		1068.0	449.0	957.0	3923.0	667.0	3929.0	5902.0	2421.0	5466.0		1779.0	1210.0	1352.0	
Elemental carbon	EC	0.09	0.08	0.06	0.10	0.09	0.09	0.18	0.08	0.15		0.16	0.11	0.13	
Organic carbon	OC	0.42	0.18	0.38	0.42	0.23	0.36	0.71	0.24	0.65		0.64	0.31	0.55	

*n.d. is not determined: proper evaluation of %PM was not possible due to the high number of concentration values <LOQ

Table S2. Total (G+P) concentrations of oxy-PAHs [pg/m³] and %PM measured in urban air of Longyearbyen in 2018.

	Cold period									Warm period				
	Dark winter P1 November-January n=8			Twilight winter P2 February n=4			Daylight spring P3 March-April n=7			%PM cold P1-P3 n=19	Polar day summer P4 May-June n=12		%PM warm P4 n=12	
	Mean	StDev	Median	Mean	StDev	Median	Mean	StDev	Median	Mean	Mean	StDev	Median	Mean
Phthalic anhydride	1796.0	689.0	1824.0	2101.0	548.0	2063.0	2542.0	621.0	2582.0	37.7	2934.0	670.0	2988.0	20.3
Benzophenone	1676.0	496.0	1650.0	4354.0	511.0	4269.0	5086.0	1413.0	5200.0	42.8	1962.0	536.0	1879.0	20.6
1-Naphthaldehyde	478.3	148.0	485.8	454.6	109.8	501.5	1157.0	587.0	1165.0	26.8	656.0	490.0	526.0	5.7
9-Fluorenone	797.7	209.9	794.7	1064.6	134.2	1030.2	1682.0	551.0	1793.0	61.4	694.1	317.4	696.1	35.1
1,2-Naphthalic anhydride	429.2	135.8	364.3	485.2	99.8	466.5	1003.0	277.0	971.0	37.9	477.0	207.8	396.8	39.5
9,10-Phenanthrenequinone	194.0	143.4	268.2	115.3	117.5	106.8	271.0	336.0	19.0	80.2	13.0	1.6	13.1	n.d.
2-Methylanthraquinone	8.1	3.2	7.7	24.4	6.0	25.8	64.7	45.8	47.8	74.5	10.4	8.5	7.8	71.8
Phthalodialdehyde	8.3	3.0	7.8	25.0	25.3	13.0	109.0	126.7	56.4	85.5	4.8	2.2	4.0	62.9
1,4-Naphthoquinone	95.3	58.6	105.0	105.0	56.4	101.1	58.6	17.0	59.4	53.2	11.9	5.4	11.0	29.2
2-Formyl-trans-cinnamaldehyde	55.7	63.5	35.0	65.1	14.2	62.0	249.8	151.3	296.3	67.9	21.8	14.9	18.1	80.3
1,2-Naphthoquinone	26.5	34.8	11.8	19.0	7.6	18.8	103.2	110.5	18.3	0.7	25.7	9.0	27.6	n.d.
1-Acenaphthenone	175.3	96.3	150.4	100.6	17.0	95.0	196.5	111.1	156.7	65.3	123.9	110.5	100.9	20.2
Biphenyl-2,2-dicarboxaldehyde	17.1	14.2	13.1	16.0	7.1	15.7	35.3	21.3	32.9	57.4	14.0	7.6	12.5	33.8
2,3-Naphthalenedicarboxilic anhydride	35.5	30.5	32.3	55.8	20.1	54.0	90.1	107.4	38.6	18.3	74.7	56.4	63.7	70.5
Anthrone	12.0	14.4	5.1	81.1	97.6	43.2	189.6	140.6	190.9	17.2	62.5	99.3	34.8	86.0
6H-Dibenzo[b,d]pyran-6-one	38.6	24.7	34.7	48.4	22.7	46.2	114.2	42.2	108.5	53.5	36.2	26.5	35.3	79.9
9,10-Anthraquinone	33.3	12.3	32.7	54.9	7.2	55.3	119.3	59.6	109.5	62.6	31.3	13.3	26.9	56.0
1,8-Naphthalic anhydride	4.8	3.4	2.9	9.6	4.9	8.0	37.1	13.6	36.9	44.0	6.4	6.4	3.5	61.7
1,4-Antraquinone	4.4	0.4	4.5	4.1	0.7	4.1	5.3	0.7	5.1	n.d.	5.5	3.1	4.3	n.d.
4,4-Biphenyldicarboxaldehyde	11.7	4.2	10.2	12.6	3.9	12.7	18.3	3.1	16.9	22.7	9.9	3.0	9.8	21.7
9-Phenanthrenecarboxaldehyde	1.2	0.6	1.0	1.3	0.5	1.0	2.6	1.4	2.9	71.1	4.9	7.6	2.8	75.8
Benzo[a]fluorenone	4.3	1.5	4.5	6.8	2.2	6.9	11.6	6.3	12.4	57.6	6.8	5.9	5.3	64.1
Benzo[b]fluorenone	3.6	1.8	2.9	6.1	1.9	5.7	11.9	6.0	9.0	55.3	4.6	3.2	4.3	65.6
Benzanthrone	6.2	3.1	5.3	9.9	2.7	10.1	24.2	14.5	22.2	71.3	9.3	7.1	8.4	79.3
1-Pyrenecarboxaldehyde	0.9	0.1	0.9	0.9	0.1	0.9	2.8	1.9	2.4	n.d.	1.5	1.5	0.9	86.5
Aceanthrenequinone	1.7	2.3	0.9	0.8	0.1	0.8	1.9	2.2	1.0	n.d.	2.5	2.5	1.0	n.d.
Benz[a]anthracene-7,12-dione	2.3	1.1	2.6	2.4	1.4	2.4	8.9	7.3	6.0	77.2	2.6	2.2	1.2	85.2
Xanthone	12.5	5.1	12.9	12.0	2.7	11.9	27.6	11.9	29.6	40.1	7.7	3.1	7.4	69.9
Acenaphthenequinone	3.6	3.0	2.8	4.7	1.1	4.6	6.0	3.3	5.7	42.9	3.6	1.7	3.0	49.4
Σ29 Oxy-PAHs	5934.0	1480.0	5482.0	9241.0	633.0	9264.0	13229.0	2681.0	14612.0		7219.0	1692.0	7717.0	

*n.d. is not determined: proper evaluation of %PM was not possible due to the high number of concentration values <LOQ

Table S3. Total (G+P) concentrations of nitro-PAHs [pg/m³] and %PM measured in urban air of Longyearbyen in 2018.

	Cold period									Warm period				
	Dark winter P1 November-January n=8			Twilight winter P2 February n=4			Daylight spring P3 March-April n=7			%PM cold P1-P3 n=19	Polar day summer P4 May-June n=12			
	Mean	StDev	Median	Mean	StDev	Median	Mean	StDev	Median	Mean	Mean	StDev	Median	Mean
1-Nitronaphthalene	11.42	7.42	10.69	14.75	7.46	12.87	21.40	14.61	17.45	9.3	2.81	1.83	2.36	1.3
2-Methyl-1-nitronaphthalene +														
1-Methyl-5-nitronaphthalene	5.29	3.64	4.85	4.05	2.83	3.32	3.42	3.32	2.26	1.4	2.23	1.28	1.74	n.d.
2-Nitronaphthalene	2.85	0.86	2.62	4.43	1.33	4.58	5.12	3.38	3.60	10.2	2.05	0.75	2.26	n.d.
2-Methyl-4-nitronaphthalene	1.48	0.82	0.97	1.16	0.47	0.95	1.15	0.19	1.16	n.d.	0.85	0.10	0.85	n.d.
1-Methyl-4-nitronaphthalene	1.95	1.81	0.96	2.77	0.80	2.62	3.94	3.49	3.17	73.8	1.12	0.68	0.85	n.d.
1-Methyl-6-nitronaphthalene	1.10	0.62	0.90	0.82	0.14	0.83	0.96	0.43	1.12	n.d.	0.98	0.47	0.86	n.d.
1,5-Dinitronaphthalene	1.13	0.64	0.93	0.85	0.14	0.85	1.10	0.14	1.05	n.d.	1.01	0.48	0.89	n.d.
2-Nitrobiphenyl	0.92	0.07	0.93	0.85	0.14	0.86	1.44	0.97	1.06	n.d.	1.02	0.51	0.88	n.d.
3-Nitrobiphenyl	2.13	0.88	2.46	1.59	1.02	1.14	2.66	2.11	1.53	4.1	1.64	0.72	1.60	n.d.
3-Nitrodibenzofuran	1.15	0.63	0.93	0.85	0.14	0.85	1.46	0.95	1.16	n.d.	1.16	0.66	0.89	n.d.
5-Nitroacenaphthene	1.31	1.08	1.32	4.31	3.93	4.30	5.65	4.33	4.75	0.8	1.35	0.77	1.20	1.3
2-Nitro-9-fluorenone	1.85	1.59	0.96	2.88	1.49	3.09	2.29	1.26	2.90	1.6	1.38	0.81	0.95	n.d.
2-Nitrofluorene	0.94	0.14	0.92	0.86	0.10	0.84	1.09	0.14	1.03	n.d.	0.86	0.11	0.86	n.d.
9-Nitroanthracene	1.32	0.96	1.00	11.74	12.66	11.09	16.92	12.55	17.67	13.2	1.00	0.32	0.92	n.d.
9-Nitrophenanthrene	1.15	0.13	1.14	6.07	2.04	6.53	3.14	2.24	2.90	3.0	1.03	0.14	1.02	n.d.
2-Nitrodibenzothiophene	0.90	0.07	0.92	0.84	0.14	0.84	1.36	0.71	1.14	n.d.	0.86	0.11	0.87	n.d.
3-Nitrophenanthrene	1.09	0.12	1.08	5.26	5.07	4.69	4.79	3.56	3.94	3.1	1.14	0.56	0.96	n.d.
2-Nitroanthracene	0.92	0.05	0.93	0.84	0.14	0.85	3.33	3.95	1.27	1.2	1.07	0.50	0.93	n.d.
9-Methyl-10-nitroanthracene	0.87	0.07	0.89	0.81	0.14	0.81	1.06	0.14	1.00	n.d.	0.83	0.10	0.84	n.d.
2-Nitrofluoranthene	1.37	0.63	1.07	1.74	1.04	1.70	2.89	0.74	3.06	65.9	0.92	0.16	0.88	n.d.
3-Nitrofluoranthene	1.09	0.09	1.11	5.75	1.41	5.27	3.85	1.29	3.89	4.2	1.46	0.78	1.07	n.d.
4-Nitropyrene	1.17	0.64	0.95	1.18	0.52	0.98	1.15	0.15	1.18	n.d.	1.05	0.61	0.90	n.d.
1-Nitropyrene	1.55	1.13	0.98	1.19	0.48	0.98	2.44	1.45	1.51	72.8	1.38	0.67	1.00	67.7
2-Nitropyrene	0.99	0.06	0.97	0.95	0.11	0.98	1.25	0.23	1.24	n.d.	0.96	0.11	0.94	n.d.
7-Nitrobenz[a]anthracene	0.94	0.06	0.94	0.86	0.14	0.86	1.37	0.87	1.06	n.d.	0.88	0.11	0.89	n.d.
6-Nitrochrysene	1.22	0.62	1.05	2.11	0.84	2.31	8.09	6.73	3.89	n.d.	0.98	0.17	0.96	n.d.
1,3-Dinitropyrene	4.47	0.48	4.46	4.38	0.43	4.43	9.01	4.20	6.14	n.d.	4.24	0.52	4.30	n.d.
1,6-Dinitropyrene	11.71	0.96	11.93	10.87	1.83	10.92	14.18	1.83	13.50	n.d.	11.20	1.37	11.24	n.d.
1,8-Dinitropyrene	11.10	0.91	11.31	10.30	1.74	10.35	13.44	1.74	12.79	n.d.	10.61	1.30	10.65	n.d.

Table S3 (continued)

	Cold period									Warm period				
	Dark winter P1 November-January n=8			Twilight winter P2 February n=4			Daylight spring P3 March-April n=7			%PM cold P1-P3 n=19	Polar day summer P4 May-June n=12			%PM warm P4 n=12
	Mean	StDev	Median	Mean	StDev	Median	Mean	StDev	Median	Mean	Mean	StDev	Median	Mean
1-Nitrobenzo[e]pyrene + 6-Nitrobenzo[a]pyrene	1.92	1.00	1.59	1.48	0.14	1.49	2.04	0.23	2.01	n.d.	1.45	0.23	1.45	n.d.
3-Nitrobenzo[e]pyrene	1.13	0.07	1.13	1.13	0.26	1.12	1.43	0.20	1.48	n.d.	1.08	0.17	1.06	n.d.
1-Nitrobenzo[a]pyrene	3.54	0.29	3.60	3.53	0.34	3.54	4.08	0.74	4.08	n.d.	3.38	0.41	3.40	n.d.
3-Nitrobenzo[a]pyrene	1.71	0.14	1.74	2.27	1.33	1.79	2.07	0.27	1.97	n.d.	1.64	0.20	1.64	n.d.
Σ35 Nitro-PAHs	83.7	18.6	78.9	113.5	13.0	116.6	149.6	34.3	131.2		65.6	9.2	66.2	

*n.d. is not determined: proper evaluation of %PM was not possible due to the high number of concentration values <LOQ

Table S4. Sampling periods and air sample volumes.

Period	Sample	Sampling start		Sampling stop		Sample volume [m ³]
		Date	Local time	Date	Local time	
P1	UNIS_1	28.11.2017	14:45	29.11.2017	14:55	342.9
P1	UNIS_2	01.12.2017	15:11	02.12.2017	16:32	353.9
P1	UNIS_3	03.12.2017	12:18	04.12.2017	10:53	318.9
P1	UNIS_4	15.01.2018	13:17	16.01.2018	15:21	392.4
P1	UNIS_5	16.01.2018	15:26	17.01.2018	15:07	350.9
P1	UNIS_6	17.01.2018	15:10	18.01.2018	15:48	368.2
P1	UNIS_7	20.01.2018	13:52	21.01.2018	12:42	352.2
P1	UNIS_8	21.01.2018	13:17	22.01.2018	15:34	417.1
P2	UNIS_9	31.01.2018	16:15	01.02.2018	16:03	410.3
P2	UNIS_10	01.02.2018	16:05	02.02.2018	22:02	485.5
P2	UNIS_11	08.02.2018	20:20	09.02.2018	21:58	324.9
P2	UNIS_12	13.02.2018	15:49	14.02.2018	21:42	364.3
P3	UNIS_13	15.03.2018	15:27	16.03.2018	13:37	256.2
P3	UNIS_14	22.03.2018	10:50	23.03.2018	13:22	312.1
P3	UNIS_15	27.03.2018	15:43	28.03.2018	15:24	283.7
P3	UNIS_16	03.04.2018	13:47	04.04.2018	16:01	370.4
P3	UNIS_17	06.04.2018	21:48	07.04.2018	20:11	335.0
P3	UNIS_18	07.04.2018	20:15	08.04.2018	22:13	369.5
P3	UNIS_19	10.04.2018	21:21	11.04.2018	15:48	257.2
P4	UNIS_20	16.05.2018	22:10	17.05.2018	21:58	356.6
P4	UNIS_21	24.05.2018	15:20	25.05.2018	16:21	344.1
P4	UNIS_22	28.05.2018	13:38	29.05.2018	15:55	397.6
P4	UNIS_23	29.05.2018	15:59	30.05.2018	16:05	369.7
P4	UNIS_24	01.06.2018	14:31	02.06.2018	22:56	476.0
P4	UNIS_25	04.06.2018	13:44	05.06.2018	16:01	420.0
P4	UNIS_26	06.06.2018	15:47	07.06.2018	16:01	361.6
P4	UNIS_27	12.06.2018	15:46	13.06.2018	23:24	439.2
P4	UNIS_28	14.06.2018	14:43	15.06.2018	13:38	319.4
P4	UNIS_29	18.06.2018	11:49	19.06.2018	15:01	400.4
P4	UNIS_30	20.06.2018	17:21	21.06.2018	16:20	315.1
P4	UNIS_31	22.06.2018	15:53	23.06.2018	18:50	380.0

Table S5. 10-day backward trajectory probability analysis data.

Period 2017/2018		Number of trajectories*	Percentage of trajectories that fit to the LRAT criteria	Median number of rain precipitation events	Median rain precipitation events efficiency, Δq , [g·kg $^{-1}$]	Median number of snow precipitation events	Median snow precipitation events efficiency, Δq , [g·kg $^{-1}$]
P1	Nov– Jan	4659	48	0	0.49	8	0.27
P2	February	1395	56	1	0.57	8	0.32
P3	March-April	2565	23	1	0.46	3	0.27
P4	May-June	2523	48	13	0.46	0	0.28

* starting at the specified height (within a source area boundary layer) over the region

Table S6. Meteorological data for sampling days.

Period	24 h sampling start Date	Ambient temperature, [°C]				Pressure, [hPa] mean	Relative humidity RH, [%] mean	Specific humidity H_{spec} , [g/kg] mean	Wind speed, [m/s]				Wind from, [degree] median	UV, [W/m²] mean
		min	max	median	mean				min	max	median	mean		
P1	28.11.2017	-14.1	-6.3	-9.7	-10.2	1012.3	68.8	1.1	0.6	6.5	3.8	3.8	113	0.8
P1	01.12.2017	-8.3	-3.4	-6.2	-6.0	989.0	83.0	1.9	0.0	7.2	1.2	1.7	113	0.4
P1	03.12.2017	-4.6	1.0	-0.1	-0.5	991.0	73.0	2.8	1.6	11.5	5.5	5.8	76	0.5
P1	15.01.2018	1.1	4.0	1.7	2.0	994.5	76.1	3.5	2.6	10.2	7.1	7.0	125	0.3
P1	16.01.2018	-0.7	1.0	0.2	0.2	1000.5	73.1	3.0	5.3	12.0	9.4	9.1	93	0.2
P1	17.01.2018	-1.6	0.6	-0.6	-0.6	1009.8	73.8	2.8	5.7	10.4	8.3	8.4	112	0.2
P1	20.01.2018	-6.5	-2.7	-4.3	-4.5	1013.1	81.6	2.1	0.2	4.8	1.6	2.0	120	0.9
P1	21.01.2018	-5.3	-1.8	-2.7	-2.7	1015.3	71.3	2.2	1.9	7.5	6.4	6.1	133	0.7
P2	31.01.2018	-16.9	-15.1	-15.4	-15.6	1024.6	57.3	0.6	3.1	7.6	6.4	6.0	136	0.8
P2	01.02.2018	-18.0	-5.5	-13.4	-12.4	1019.7	65.6	1.0	0.6	7.2	4.2	4.1	118	0.3
P2	08.02.2018	-9.8	1.2	-2.7	-3.2	993.3	67.3	2.0	2.6	10.6	7.7	7.3	126	0.6
P2	13.02.2018	-8.4	-4.3	-5.7	-5.9	1012.4	72.7	1.7	6.0	13.2	10.8	10.4	126	0.7
P3	15.03.2018	-9.9	-6.1	-7.4	-7.6	1019.4	71.9	1.4	3.6	10.1	7.5	7.2	122	18.4
P3	22.03.2018	-15.9	-10.3	-11.6	-12.9	1007.1	61.4	0.8	1.2	8.4	3.4	4.5	284	120.1
P3	27.03.2018	-13.3	-9.4	-11.0	-11.2	1006.0	75.2	1.1	1.0	7.0	3.8	3.9	125	91.0
P3	03.04.2018	-16.4	-12.8	-14.8	-14.7	1024.7	57.7	0.7	7.2	11.8	9.7	9.7	129	186.5
P3	06.04.2018	-17.1	-9.8	-15.1	-14.4	1018.6	53.6	0.6	0.6	5.9	1.9	2.7	125	207.9
P3	07.04.2018	-17.0	-7.5	-12.6	-12.7	1016.5	66.3	0.9	0.6	6.2	2.7	2.8	116	163.1
P3	10.04.2018	-12.6	-4.7	-8.6	-8.3	1006.7	68.5	1.4	2.7	7.9	5.2	5.2	124	166.6
P4	16.05.2018	3.8	5.6	4.9	4.7	999.6	68.4	3.9	6.7	16.7	11.5	11.8	91	145.9
P4	24.05.2018	-0.1	4.5	1.9	1.7	1008.5	75.1	3.5	2.3	10.4	5.2	5.5	228	262.4
P4	28.05.2018	1.3	4.2	2.9	2.7	1014.4	73.5	3.6	1.9	11.4	7.1	7.3	102	202.5
P4	29.05.2018	1.1	4.4	1.9	2.2	1021.1	80.2	3.7	0.4	5.5	3.3	3.2	302	158.7
P4	01.06.2018	1.5	5.0	3.2	3.4	1000.7	80.9	4.1	0.5	8.0	3.1	3.3	292	134.6
P4	04.06.2018	1.1	3.5	1.9	2.1	1013.8	69.9	3.3	0.6	9.5	6.5	5.8	112	174.5
P4	06.06.2018	2.8	4.3	3.4	3.4	1003.7	66.5	3.5	2.6	9.2	5.4	5.8	294	366.4
P4	12.06.2018	0.3	2.3	1.6	1.5	998.9	72.3	3.3	1.6	6.2	4.6	4.2	304	186.2
P4	14.06.2018	3.0	5.7	3.7	4.1	1006.2	60.8	3.4	0.5	11.8	3.9	5.2	120	272.8
P4	18.06.2018	4.9	7.0	6.3	6.2	1005.6	62.2	4.0	2.3	13.7	7.9	7.6	116	275.4
P4	20.06.2018	5.1	6.5	5.8	5.8	1006.8	84.5	5.0	1.8	5.7	3.8	3.6	304	178.9
P4	22.06.2018	3.0	9.3	6.2	5.4	1010.5	92.2	5.1	0.8	7.1	3.0	2.9	313	301.6

Table S7. PAH concentrations (G+P; pg/m³) in the air of Longyearbyen (UNIS) compared to the levels at the background Arctic stations in Svalbard and Finland measured during the same period in 2017/2018. The determined periods are November-January (P1), February (P2), March-April (P3), and May-June (P4).

N of compounds	Location	Coordinates	Period	N samples	Mean	SD	Minimum	Median	Maximum
$\Sigma 20^*$ PAHs	Zeppelin, Svalbard		P1	9	736	357	275	742	1227
	Zeppelin, Svalbard	78°58' N, 11°53' E, 474 m asl	P2	4	411	105	297	397	551
	Zeppelin, Svalbard		P3	6	141	42	88	151	191
	Zeppelin, Svalbard		P4	10	72	21	46	69	111
$\Sigma 20$ PAH	UNIS, Svalbard		P1	8	951	388	477	863	1573
	UNIS, Svalbard	78.22° N, 15.65° E, 25 m asl	P2	4	3173	656	2797	2871	4155
	UNIS, Svalbard		P3	7	4351	2037	1829	4659	6611
	UNIS, Svalbard		P4	12	1657	1110	626	1311	4198
$\Sigma 11^{**}$ PAHs	Pallas, Finland		P1	3	1102	92	999	1131	1176
	Pallas, Finland	68°00' N, 24°14' E, 340 m asl	P2	-	-	-	-	-	-
	Pallas, Finland		P3	2	341	156	231	341	452
	Pallas, Finland		P4	3	209	65	136	230	261
$\Sigma 11$ PAH	UNIS, Svalbard		P1	8	488	209	239	474	847
	UNIS, Svalbard	78.22° N, 15.65° E, 25 m asl	P2	4	2217	730	1546	2033	3255
	UNIS, Svalbard		P3	7	2428	1266	905	3073	3597
	UNIS, Svalbard		P4	12	978	742	286	732	2725

Data acquired from <http://ebas.nilu.no>, last access: 20 December 2020

*Summed compounds are 1-MeNap, 2-MeNap, Ace, Flu, Phe, Ant, Flt, Pyr, BaAnt, Chry, Ret, BePyr, BjFlt, BbFlt, BkFlt, BaPyr, DBAnt, BghiP, IPyr, Cor

**Summed compounds are Ant, BaAnt, BaPyr, BbFlt, BghiP, BkFlt, Chry, DBAnt, Flt, Phe, Pyr

Figure S1. Maps of the Arctic (**a**), Svalbard (**b**), vicinity of Longyearbyen (**c**), and marine traffic in Isfjorden (**d**) (North-West to the UNIS sampling station).

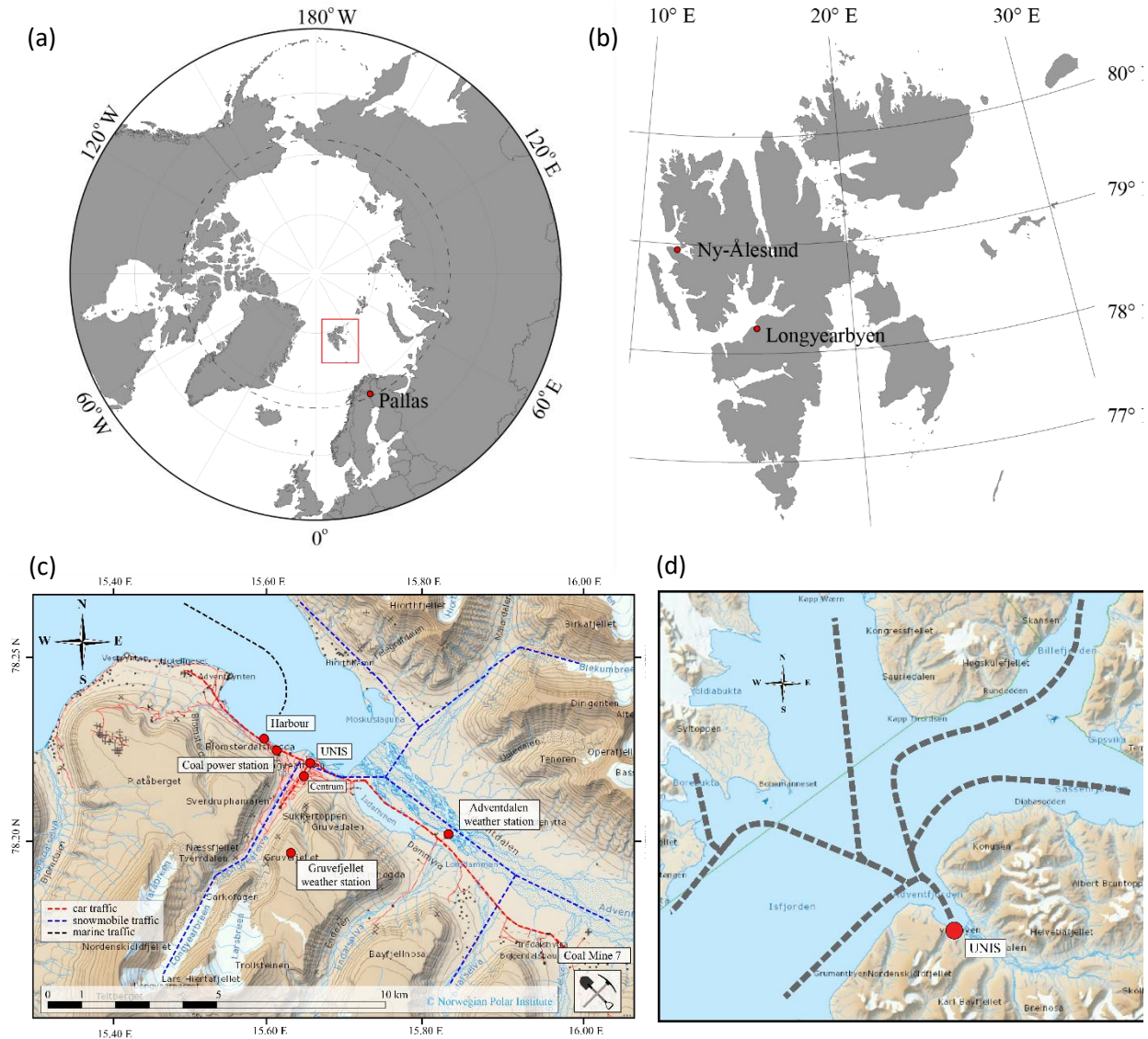


Figure S2. Sun diagram for Longyearbyen.

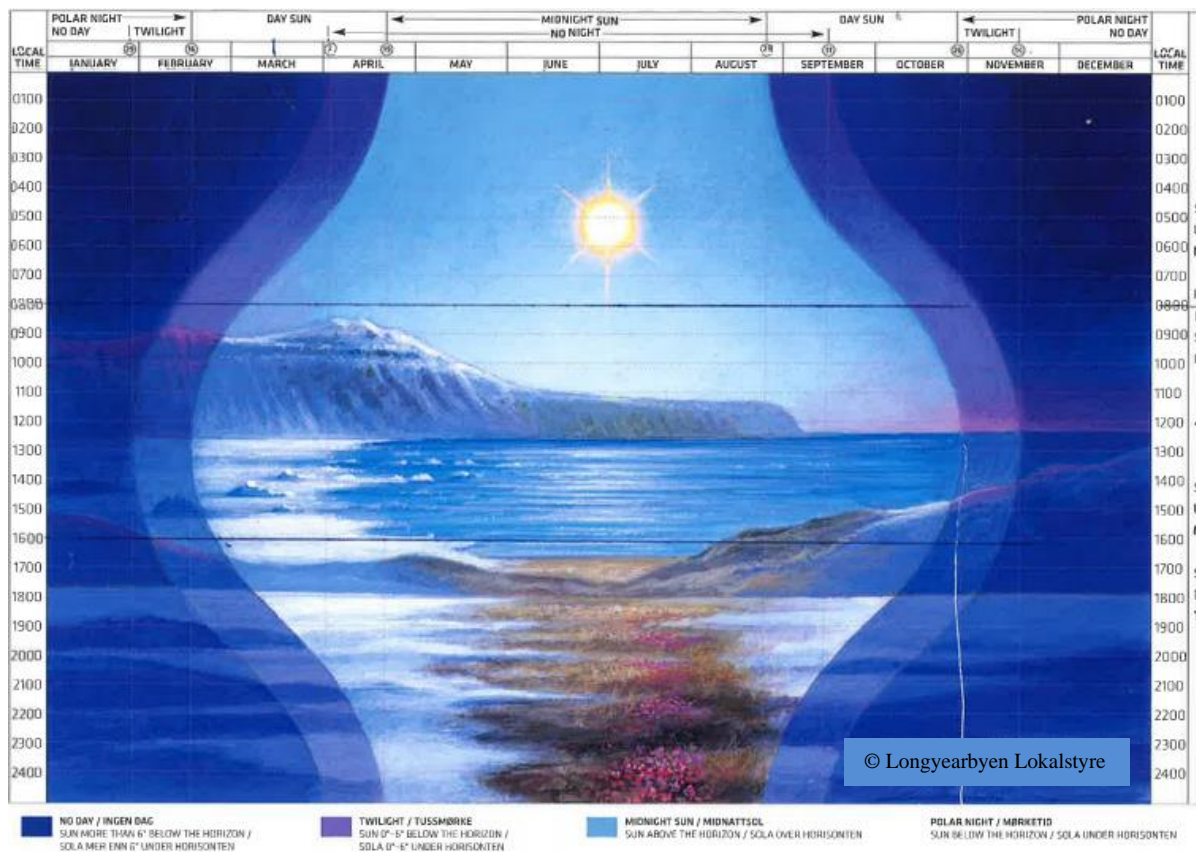
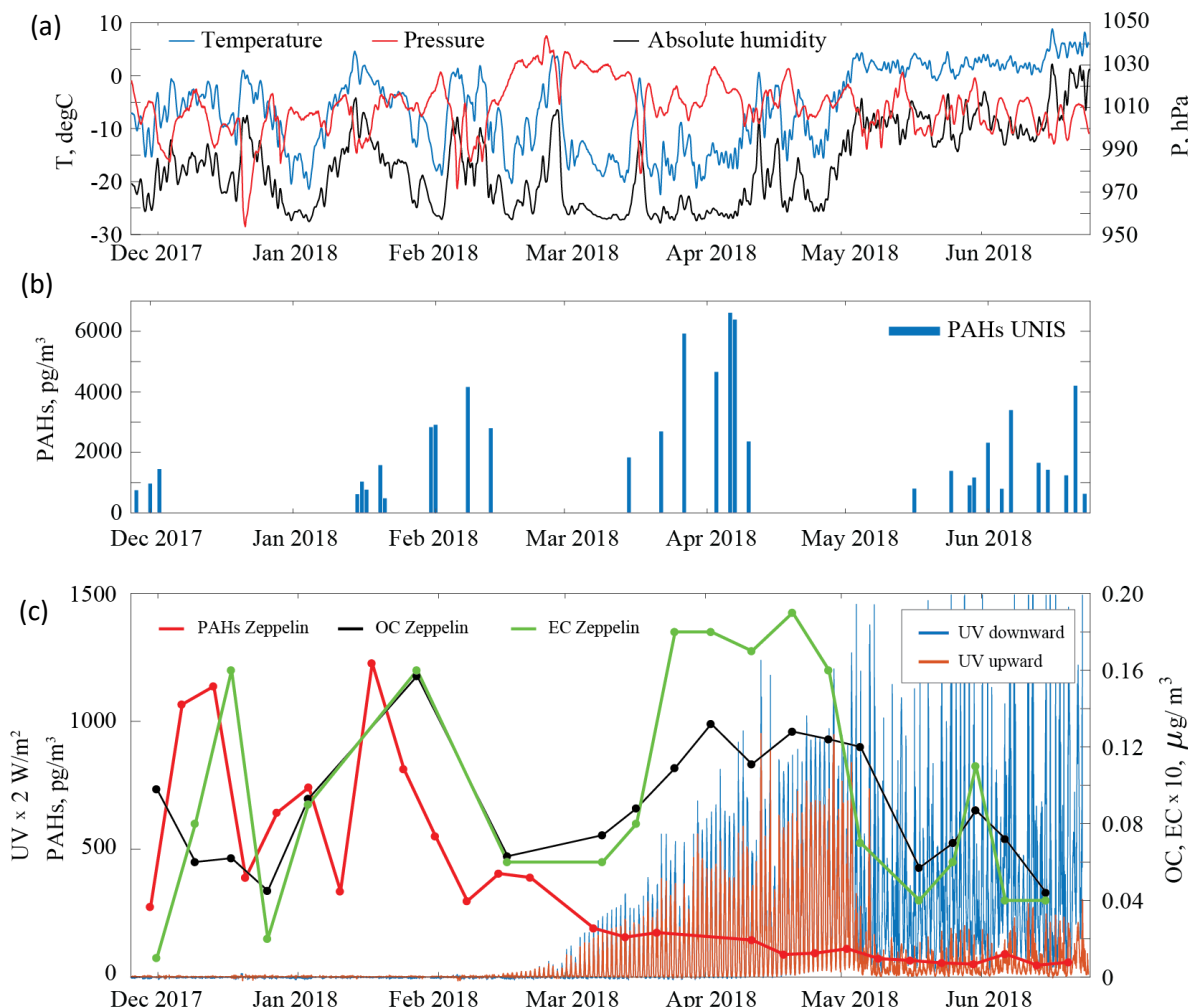
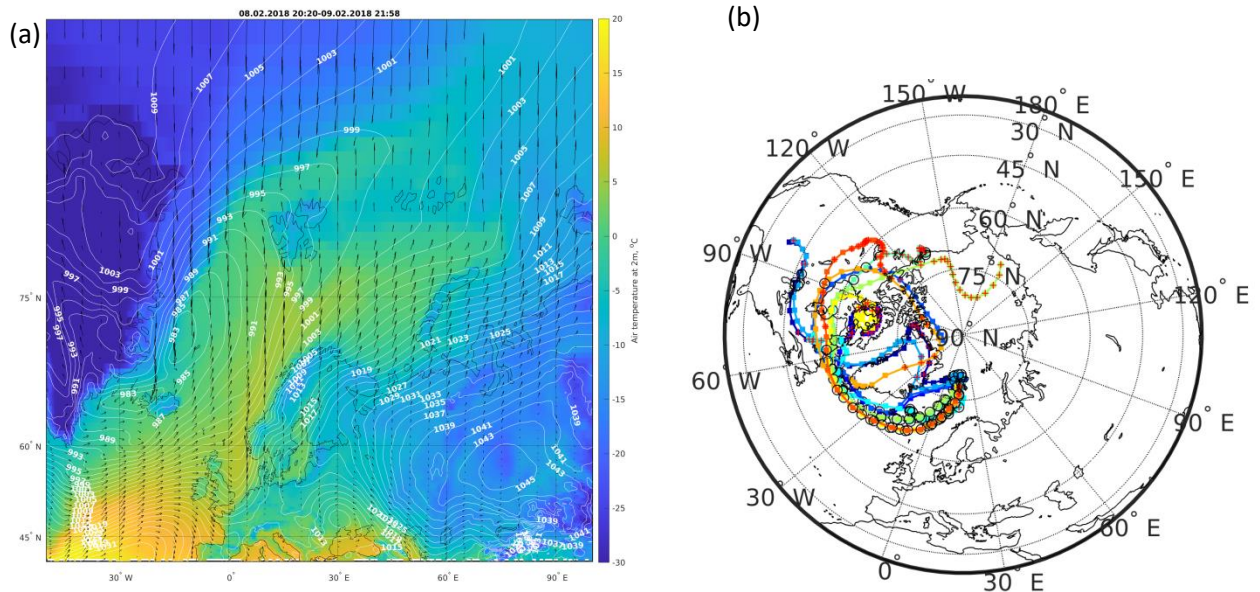


Figure S3. Seasonal trends of weather parameters (a) and \sum_{20} PAH* total (G+P) concentrations measured in Svalbard air in 2018 at UNIS (Longyearbyen; urban) (b) and Zeppelin (Ny-Ålesund; background) (c) stations.



*Summed compounds are 1-MeNap, 2-MeNap, Ace, Flu, Phe, Ant, Flt, Pyr, BaAnt, Chry, Ret, BePyr, BjFlt, BbFlt, BkFlt, BaPyr, DBAnt, BghiP, IPyr, Cor

Figure S4. Synoptic map (a) and 10-day backward trajectories (b) illustrating frequent winter events of the Atlantic warm air masses transport to the Arctic.



Note: An ambient temperature increase of 13.3 °C was registered during the 24 h of air sampling in Longyearbyen started on the 8th of February 2018 (the example on the plots).

Figure S5. Wind rose diagrams typical for the P1-P3 cold (**a**) and P4 summer (**b-c**) periods.

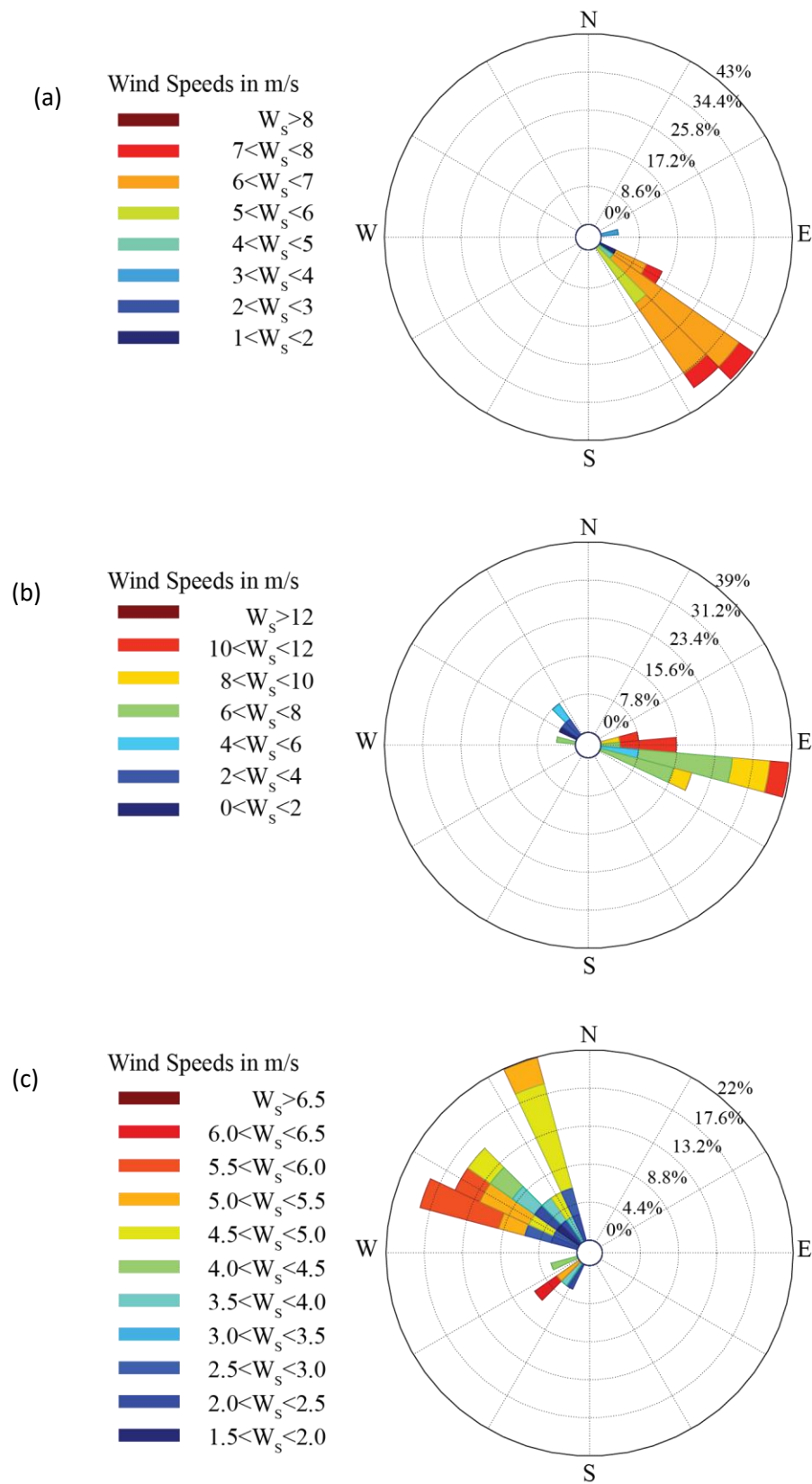


Figure S6. Correlations of the OC/EC ratio and the sum gross tonnage (dimensionless) of vessels arriving and departing the harbour of Longyearbyen during sampling hours on summer days when the UNIS station was downwind the harbour (P4; n=7).

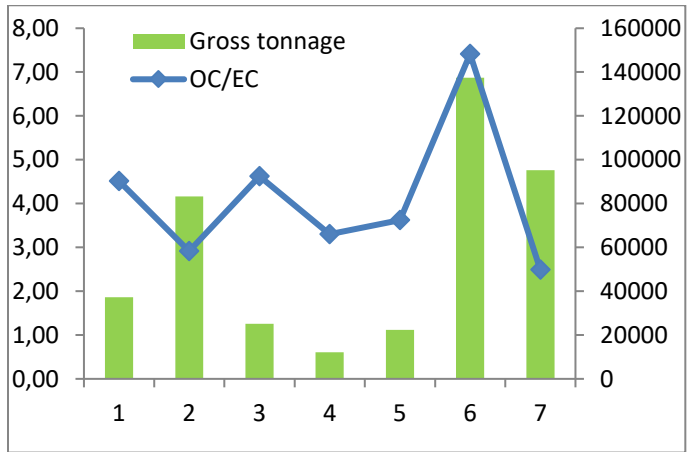


Figure S7. Comparison of the P1-P3 cold period profiles of PAHs based on the snowmobile traffic intensity.

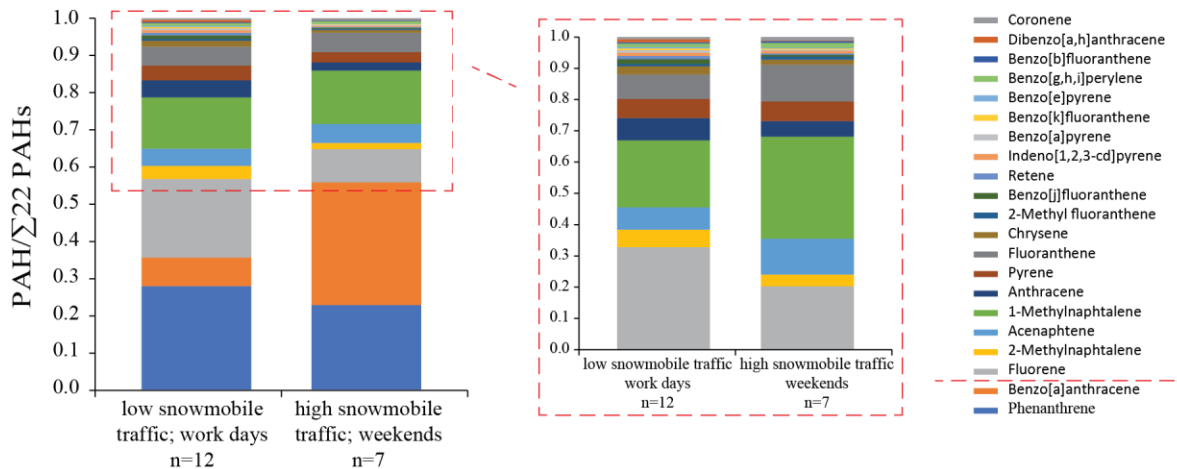
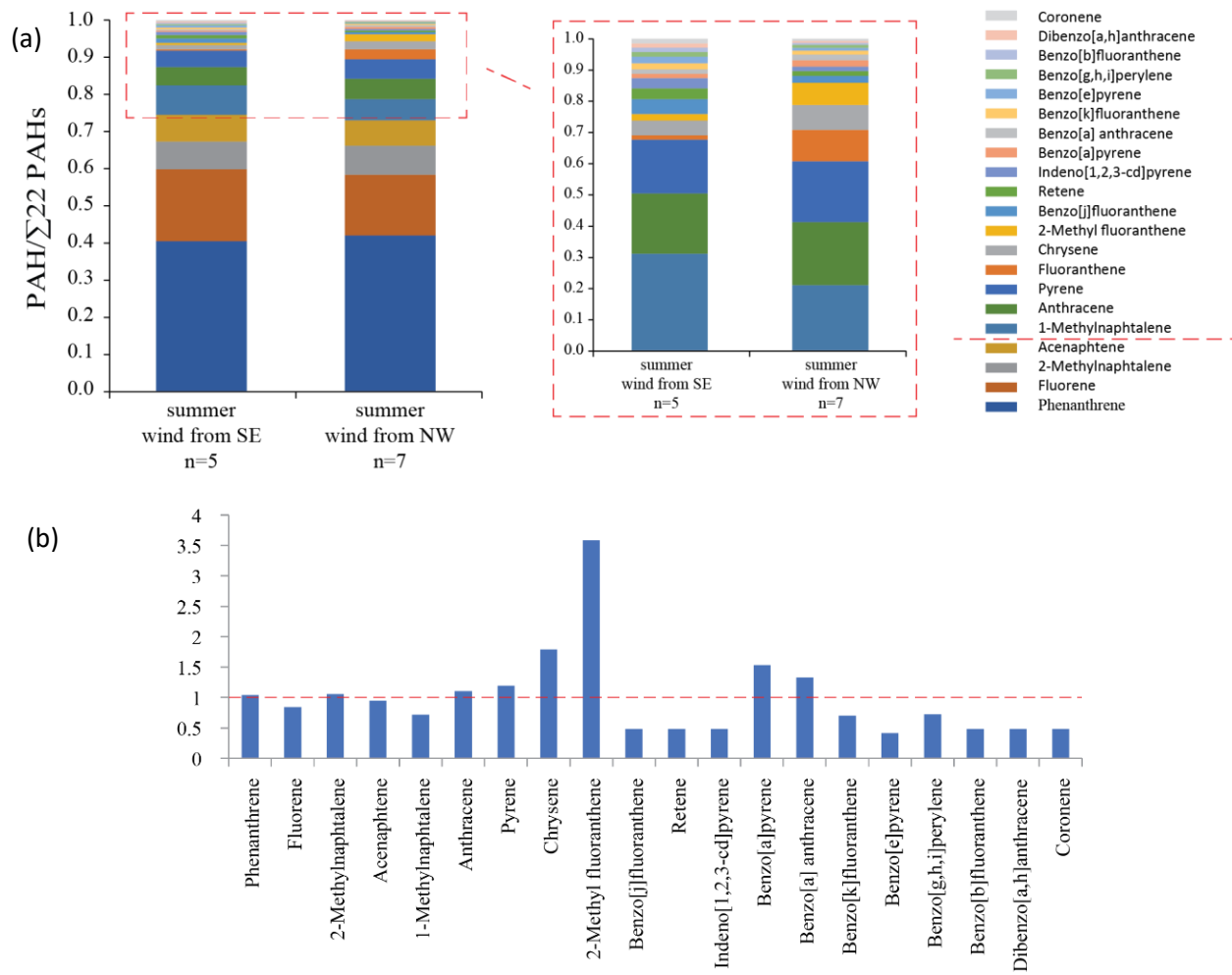
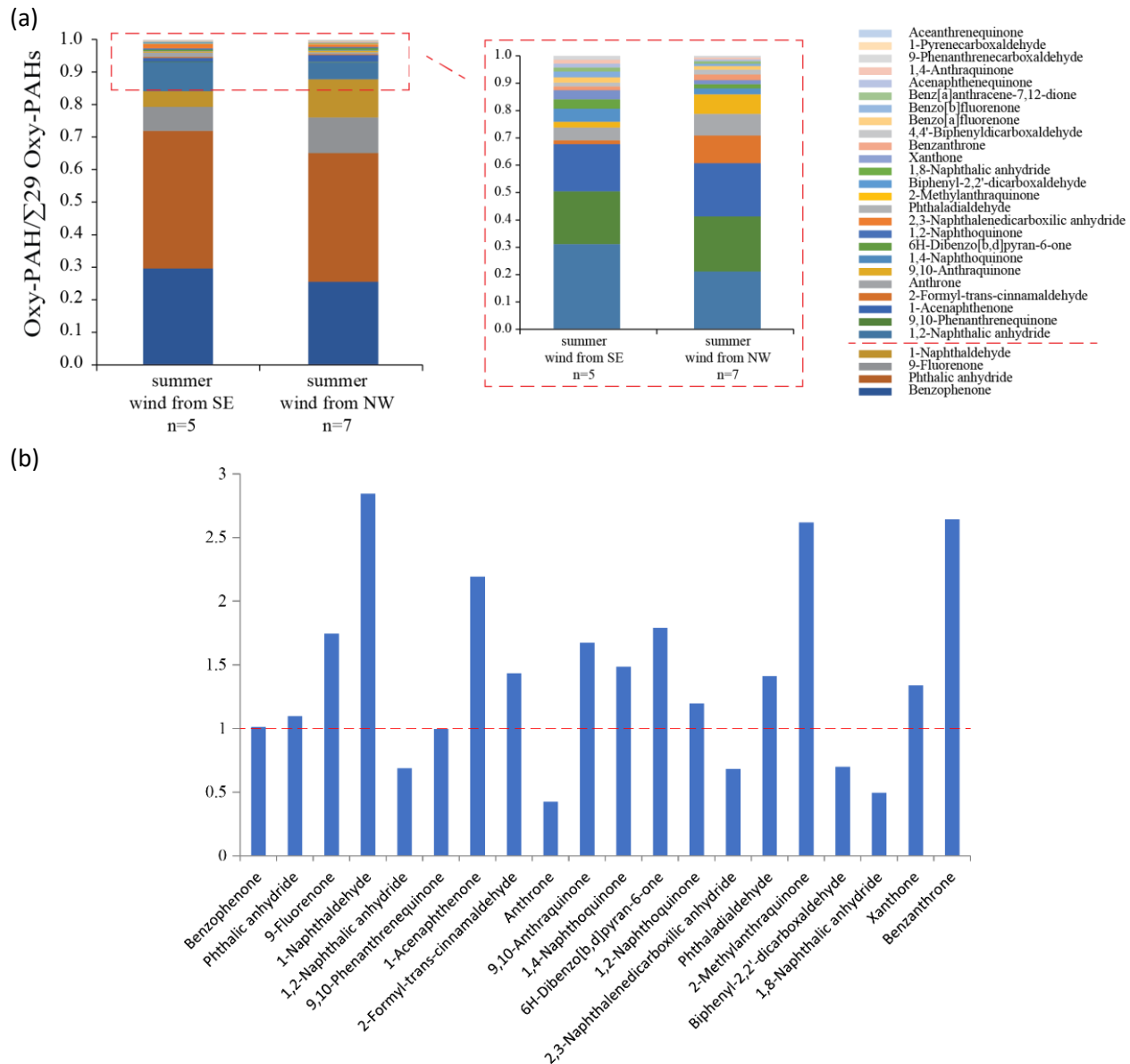


Figure S8. Comparison of the P4 summer profiles of PAHs based on wind direction (a) and the chemical profile proportion increase rates of PAHs (b) as result of ship traffic (NW wind) in the harbour of Longyearbyen.



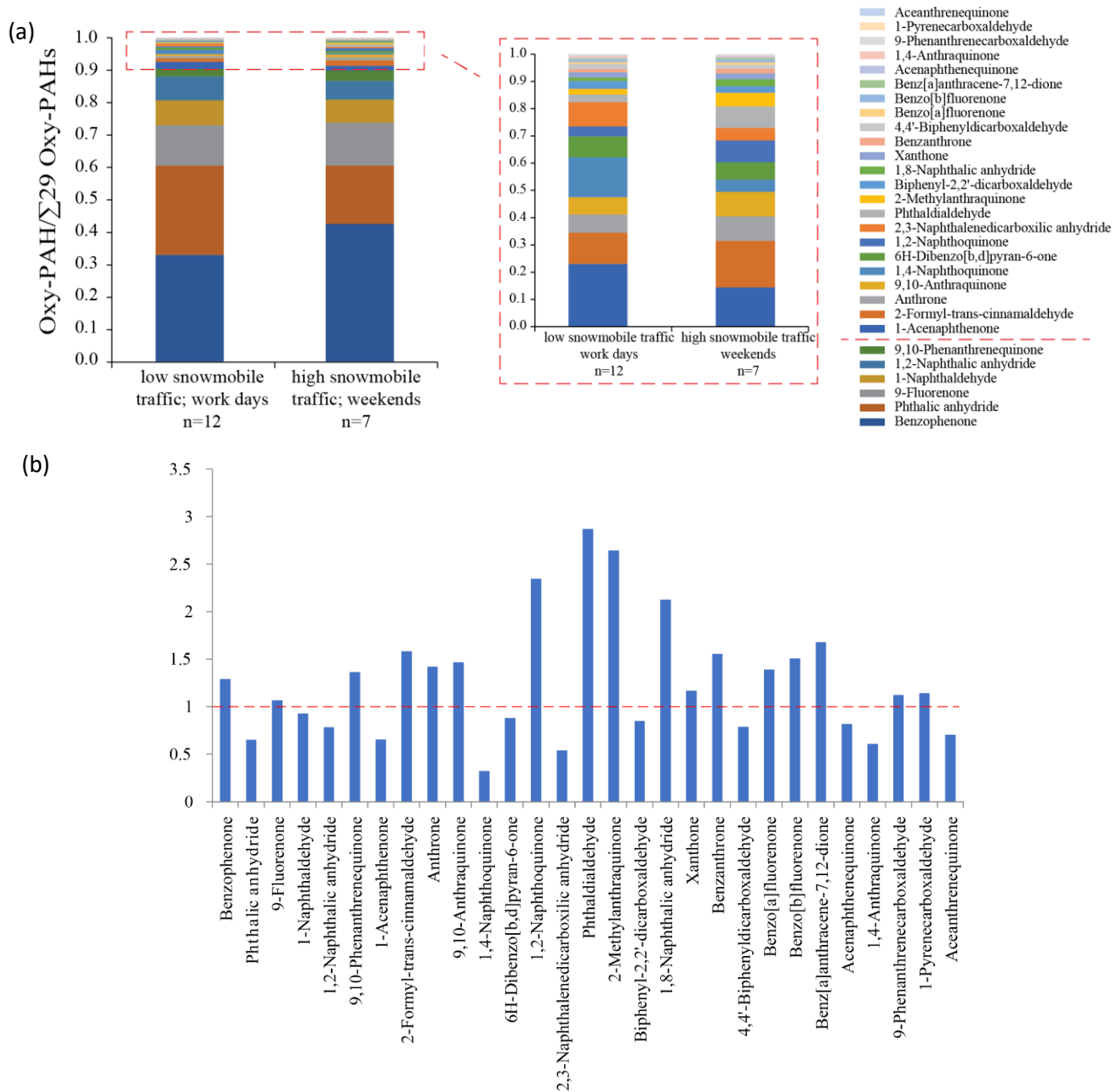
Note: The proportion increase rate of Flt (7.5) is not included to scale the picture. Rate >1 indicates enhanced rate of increase of a compound proportion in the total PAHs profile on the days with NW wind from the harbour

Figure S9. Comparison of the P4 summer profiles of oxy-PAHs based on wind direction (**a**) and the chemical profile proportion increase rates of selected oxy-PAHs (with concentration > 10 pg/m³) (**b**) as result of ship traffic (NW wind) in the harbour of Longyearbyen.



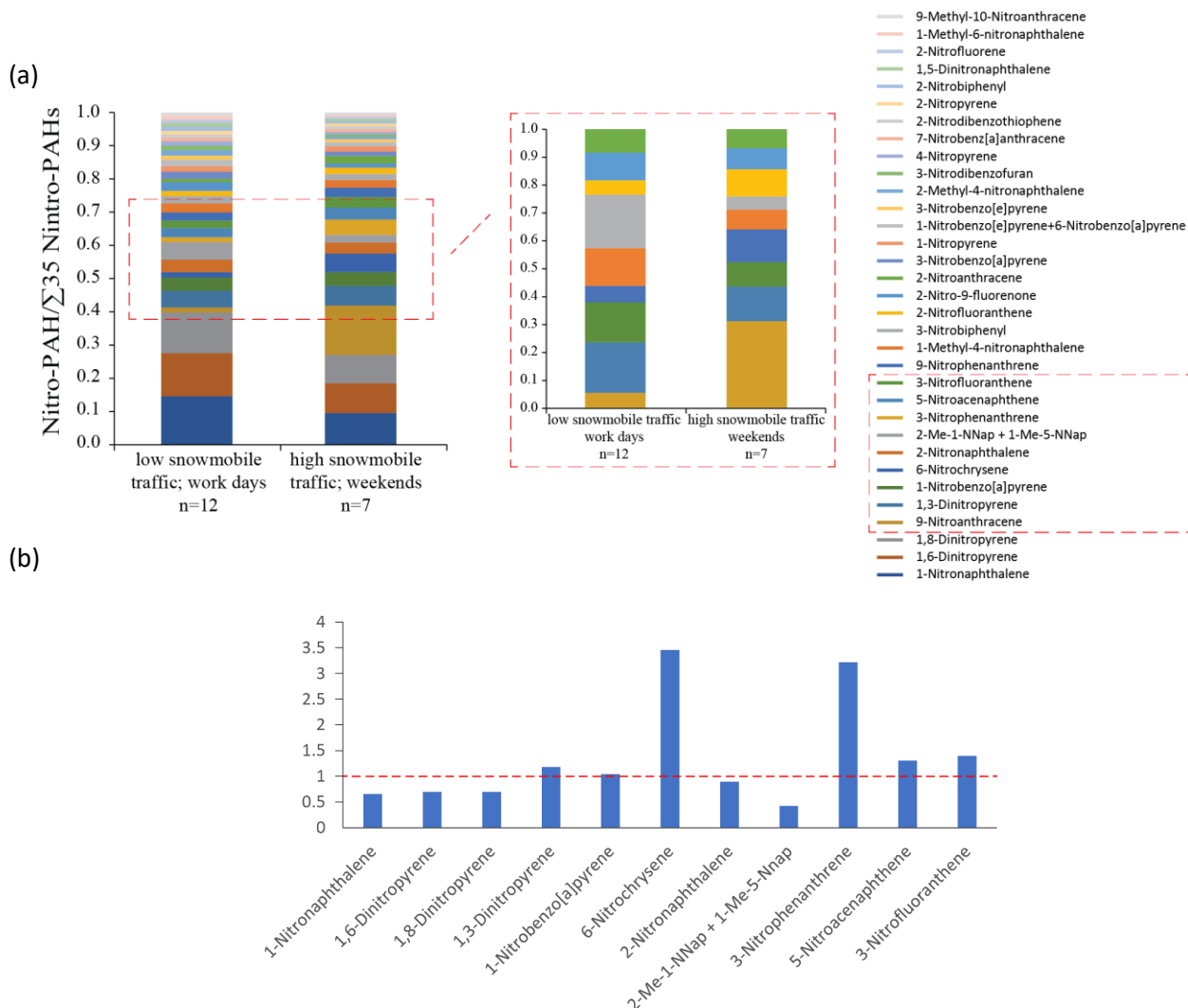
Note: Rate >1 indicates enhanced rate of increase of a compound proportion in the total oxy-PAHs profile on the days with NW wind from the harbour

Figure S10. Comparison of the cold period P1-P3 profiles of oxy-PAHs based on snowmobile traffic intensity (a) and the chemical profile proportion increase rates of selected oxy-PAHs (with concentration > 10 pg/m³) (b).



Note: Rate >1 indicates enhanced rate of increase of a compound proportion in the total oxy-PAHs profile compared to the days with low or no snowmobiles driving.

Figure S11. Comparison of the cold period P1-P3 profiles of nitro-PAHs based on the snowmobile traffic intensity (a) and the chemical profile increase rates of selected nitro-PAHs (b).



Note: The proportion increase rate of 9-nitroanthracene (9.6) is not included to scale the picture. Rate >1 indicates enhanced rate of increase of a compound proportion in the total nitro-PAHs profile compared to the days with low or no snowmobiles driving